Chinese Chemical Letters 34 (2023) 107830

Contents lists available at ScienceDirect

Chinese Chemical Letters

journal homepage: www.elsevier.com/locate/cclet

Low-molecular-weight supramolecular adhesive with resistance to low temperatures

Shuanggen Wu[a], Wenbo Wang[a], Changyong Cai[a], Fenfang Li[b], Shengyi Dong[a,*]

[a] College of Chemistry and Chemical Engineering, Hunan University, Changsha 410082, China
[b] College of Chemistry and Chemical Engineering, Central South University, Changsha 410083, China

ARTICLE INFO

Article history:
Received 20 June 2022
Revised 7 September 2022
Accepted 14 September 2022
Available online 17 September 2022

Keywords:
Supramolecular adhesive
Low temperature resistance
Underwater adhesion
Low-molecular-weight monomer
Supramolecular adhesion

ABSTRACT

The design of adhesive materials with strong adhesion capacity at low temperatures is a great challenge. Herein, we report a low-molecular-weight supramolecular adhesive that exhibits good adhesion performance to various surfaces at low temperatures (from −18 °C to −80 °C). Moreover, this supramolecular adhesive has good adhesion ability in the presence of water.

Over the past decade, supramolecular adhesives have triggered a flurry of attentions in material science and supramolecular chemistry [1–5]. Non-covalent bonding in structures endows adhesive materials with various dynamic and reversible features [6–10]. Nowadays, supramolecular adhesives have become an important member of the high-performance adhesive family [11–18].

In the application of supramolecular adhesives, low temperatures play a significant role in the adhesion effect and performance [19,20]. It is well-known that high temperature can destroy the non-covalent interactions and supramolecular structures, thus greatly weakening the adhesion strength [21–24]. However, the negative effect of low temperatures on adhesion is frequently ignored, as low temperatures can enhance the binding capacity of supramolecular pairs [25,26]. As a matter of fact, low temperatures dramatically affect the integrity of adhesion layers, and cause the debonding between surfaces and adhesive materials [27–30]. Different anti-freeze molecules, such as salts and alcohols, have been used in the preparation of adhesive materials to yield low temperature-resistance [31,32]. However, low-temperature-resistant supramolecular adhesives without any anti-freeze components are still limited [33–36].

Herein, we report a serendipitously found supramolecular adhesive that exhibits good adhesion effects to various surfaces at low temperatures. Strong and tough adhesion performances of supramolecular adhesive on metal, glass, polymethyl methacrylate (PMMA), and polytetrafluoroethylene (PTFE) were observed, when temperatures were below freezing point. At extremely low temperatures (< −40 °C), stable adhesion was still realized.

During the synthesis of bis(**B21C7**)-substituted **ZE** [37], a wrong molar ratio of **B21C7-NH2** and acid (1:1) was applied (Scheme 1). Firstly, a labile intermediate compound (*O*-acylisourea ester) was formed *via* the reaction of EDC with the carboxyl group of **TA**. Secondly, **B21C7-NH2** partially substitutes the EDC group of *O*-acylisourea ester *via* a nucleophilic attack to produce amide. Finally, the residual EDC groups of *O*-acylisourea ester may undergo cyclic electronic displacement (N→O displacement) to generate *N*-acylurea (Fig. S1 in Supporting information) [38]. Therefore, **OE** instead of **ZE** was monitored and isolated. Compared with **ZE** and **TE**, **OE** is a glue-type material with high viscosity and poor fluidity (Fig. 1a), as confirmed by various rheology measurements. As shown in Fig. 1e and Figs. S25-S27 (Supporting information), **OE** displays excellent temperature-dependent rheological behavior, which can be attributed to the bulk state and thermal stable feature of **OE**. In addition, the composite viscosity of **OE** was increased by 10^5 times as the testing temperature decreased from 80 °C to 10 °C, and this rheological behavior was reversible (Fig. 1e). This observation can be ascribed to the existence of dynamical non-covalent interactions in the system, such as hydrogen bonding, van der Waals forces, and F–F interactions. In contrast, neither **ZE** nor **TE** exhibits any viscosity in a wide temperature range (from −80 °C to 100 °C). In our previous studies, it has been demonstrated that benzo-21-crown-7 is essential to realize strong adhesion [39–41]. Thus, **TE** did not show any adhesion property due

* Corresponding author.
E-mail address: dongsy@hnu.edu.cn (S. Dong).

https://doi.org/10.1016/j.cclet.2022.107830
1001-8417/

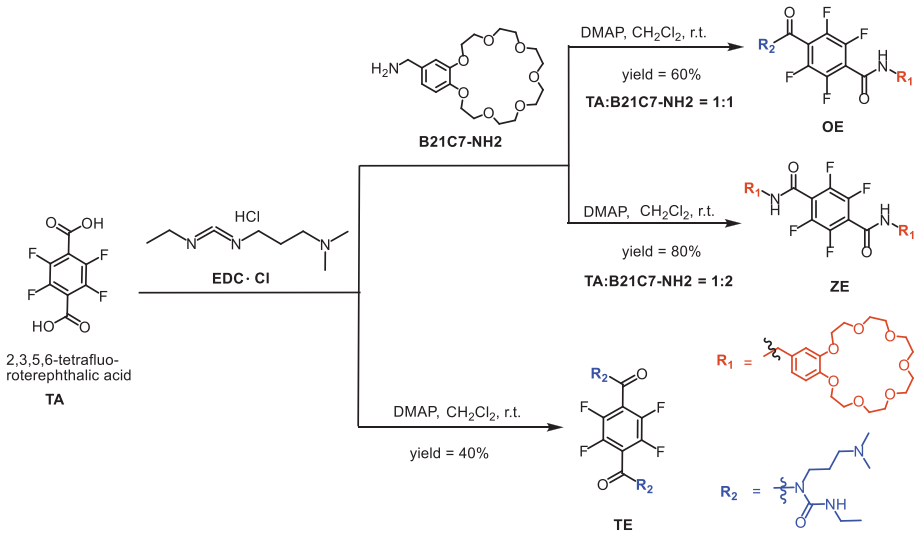

Scheme 1. Synthetic routes of **OE**, **ZE**, and **TE**.

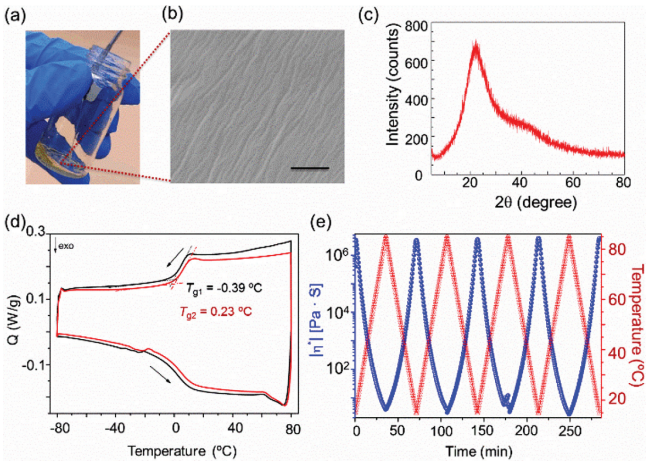

Fig. 1. Characterization of **OE**. (a, b) Macroscopic and SEM image of **OE** (scale bar is 10 μm). (c) PXRD pattern of **OE**. (d) DSC spectra of **OE**. (e) Temperature-dependent reversible composite viscosity of **OE**.

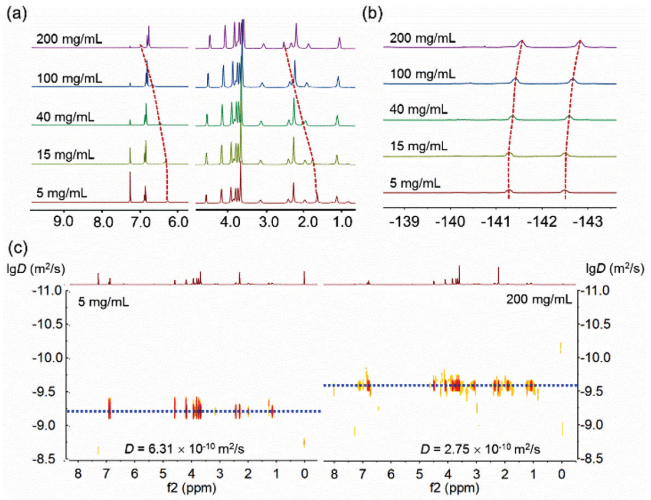

Fig. 2. (a) Partial concentration-dependent ^{1}H NMR spectra of **OE** ($CDCl_3$, 400 MHz, room temperature). (b) Partial concentration-dependent ^{19}F NMR spectra of **OE** ($CDCl_3$, room temperature). (c) Concentration-dependent DOSY NMR spectra of **OE** ($CDCl_3$, 600 MHz, room temperature).

to the absence of the crown ether ring [41]. Meanwhile, as a 1,4-disubstituted compound, **ZE** favors aggregating together (strong cohesion), which dramatically attenuated the adhesion capacity to surfaces (weak adhesion) [41].

Based on above information, more investigations were carried out to study the physicochemical and mechanical properties of **OE** (Figs. S2-S24 in Supporting information). Only a wide peak was observed in powder X-ray diffraction (PXRD) pattern, demonstrating the amorphous nature of **OE** (Fig. 1c). Scanning electron microscopy (SEM) tests showed a dense, non-porous morphology of **OE**, without the existence of three-dimensional fibers (Fig. 1b and Fig. S23). A low glass transition temperature (T_g of 0.23 °C) close to the freezing point was recorded in differential scanning calorimetry (DSC) measurements, indicating the potential low-temperature adhesion application of **OE**. Meanwhile, during the heating-cooling cycles, a similar T_g (−0.39 °C) was found in the second heat-cooling cycle (Fig. 1d).

With the above information in mind, the driven force of supramolecular adhesion was studied (Figs. S9−S20). As shown in Fig. 2, concentration-dependent ^{1}H NMR spectra, concentration-dependent ^{19}F NMR spectra, and concentration-dependent two-dimensional diffusion ordered NMR (DOSY) spectra are obtained to study the interaction between **OE**. No new covalent interaction was found in either diluted or concentrated **OE** solutions [39–41]. Meanwhile, as shown in Fig. 2a, the signals of NH protons H on **OE** moved down-field, from 6.27 ppm to 6.97 ppm, when the concentration of **OE** was increased from 5 mg/mL to 200 mg/mL, suggesting that the existence of hydrogen bonding among the amide groups (the amide groups act as H-bonding acceptors and donors simultaneously). In addition, the chemical shift of fluorine moved to the high field when the concentration of **OE** was increased from 5 mg/mL to 200 mg/mL (Fig. 2b), indicating that the existence of F–F interaction [38].

Moreover, by analyzing the DOSY NMR spectra of **OE**, two diffusion coefficients (D) of 6.31×10^{-10} m^2/s (5.0 mg/mL, 1.28 nm) and 2.75×10^{-10} m^2/s (200 mg/mL, 2.95 nm) were observed, respectively, suggesting the concentration-dependent aggregation of **OE**. Combining with results from macroscopic tests and rheological experiments, it is reasonable that **OE** forms high molecular weight species at concentrated solutions and in bulk state, based on the reversible non-covalent interactions.

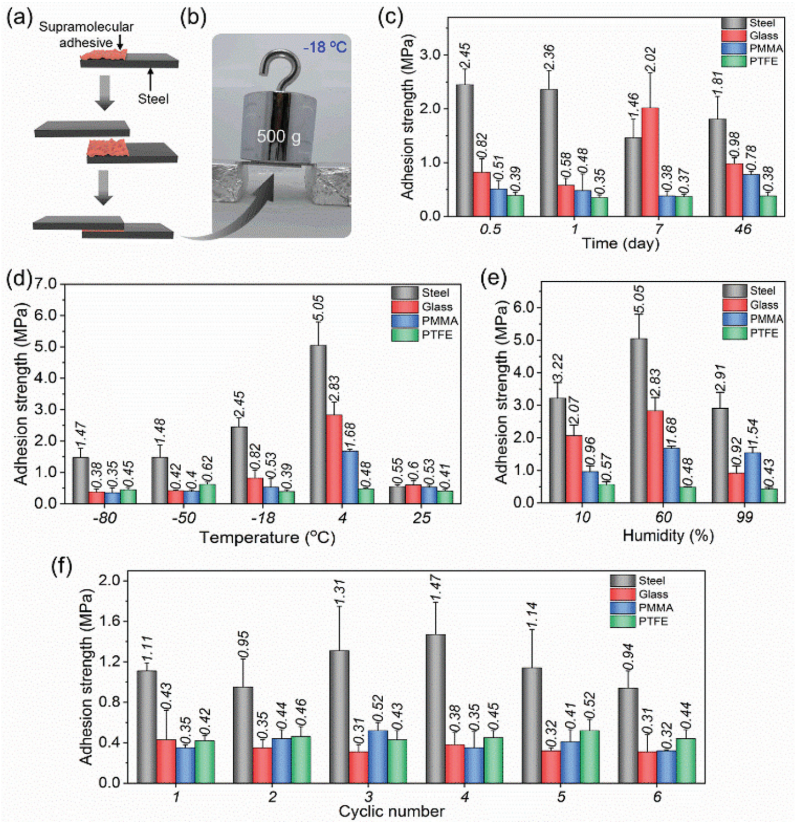

Fig. 3. Adhesion performance of **OE** at low temperatures. (a) Adhesion process of **OE**. (b) **OE**-steel system hung with a weight of 500 g. (c) Adhesion strengths of **OE** at −18 °C for different time. (d) Adhesion strengths of **OE** at various temperatures (−80 °C, −50 °C, −18 °C, 4 °C, and 25 °C) for 12 h. (e) Adhesion strengths of **OE** at 4 °C under various relative humidities (10%, 60%, and 99%) for 12 h. (f) Cycle measurements of **OE** at −18 °C.

As a glue-like material, **OE** showed a good processability (Fig. 1a). Uniform, thin, and intact adhesion layer can be easily cast on various surfaces, including steel, glass, PMMA and PTFE. As shown in Fig. 3a, two steel plates are firmly cohered together by **OE**, without any tedious operations or additives. In the following weight-loading tests, no failure of the adhesion or destruction of the adhesive layer was observed (Fig. 3b). Low testing temperatures (from 25 °C to −18 °C) did not affect the macroscopic adhesion effect of **OE**. As a matter of fact, **OE** exhibited better adhesion performances at low temperatures (such as 4 °C and −18 °C) than that at 25 °C. The information clearly demonstrate that **OE** has great potential as a powerful low-temperature-resistant adhesive material [30,42,43].

Lap-shear measurements were later carried out to quantitatively evaluate the adhesion effect of **OE** (Figs. 3c-e). Compared with the adhesion strength of **OE** obtained at 25 °C, stronger adhesion capacities of **OE** were realized at low temperatures. For example, moderate adhesion strengths (0.41−0.6 MPa) of **OE** to four tested surfaces were recorded at 25 °C, while adhesion strength of **OE** up to 5.05 MPa (steel) was obtained at low testing temperature (4 °C). As shown in Fig. 3d, 4 °C is the optimum temperature for the supramolecular adhesion of **OE**. This observation can be attributed to glass transition behavior of **OE** (T_g close to 0 °C).

Tough, long-term adhesion of **OE** at low temperatures (such as −18 °C) was successfully realized. As shown in Fig. 3c, good adhesion effects of **OE** to glass, PMMA, and PTFE, were observed, indicating the potential application of **OE** as a long-last low temperature-resistant adhesive. After adhering to steel for 46 days, only a moderate decrease in adhesion strength was found, from 2.45 MPa to 1.81 MPa (Fig. 3c). The adhesion effects of **OE** between −4 °C and −80 °C demonstrate the strong adhesion capacity of **OE** at low temperatures. Compared with crown ether-based supramolecular adhesives, **OE** exhibited stronger adhesion effect at long-time adhesion tests [37,39–41].

Humidity plays an important role in the adhesion performance of **OE**. **OE** showed the strongest adhesion strengths to steel (5.05 MPa) and glass (2.83 MPa) at RH 60% and 4 °C (Fig. 3e). Either elevating or decreasing RH% obviously weakened the adhesion effects of **OE** (4 °C). A possible explanation is that water molecules can participate in the supramolecular polymerization and adhesion, *via* the hydrogen bonding formation with **OE** (crown ether unit) and/or adhered surface [31,39,40,44]. Therefore, high or low content of water may interfere with the assembly pattern of **OE**.

After multiple cycle measurements at low temperatures (Fig. 3f), no obvious decay or fatigue of adhesion capacity of **OE** on testing substrates was observed, indicating that **OE** can be used as a recyclable adhesive material. For example, after seven cycles, the adhesion strengths of **OE** to steel and glass were about 84.7% (0.94 MPa) and 72.1% (0.31 MPa) of that of the first time, respectively (Fig. 3f). A possible explanation is that the non-covalent interactions, such as hydrogen bonds, could be weakened upon heating and reconstructed at low temperatures [45–50]. Moreover, compared to the glass without the treatment of **OE**, no obvious changes of contact angel and FTIR were observed from the glass with the treatment of **OE** (Figs. S30 and S31 in Supporting information). Meanwhile, the ^{1}H NMR spectrum of **OE** coated on a glass surface for 48 h is the same as that of freshly obtained **OE** (Fig. S32 in Supporting information). These results suggested that **OE** did not participate in the covalent bonding with the surface of the materials.

Interestingly, **OE** exhibited strong affinity to steel at extremely low temperatures. As shown in Fig. 4a, two steel plates are firmly

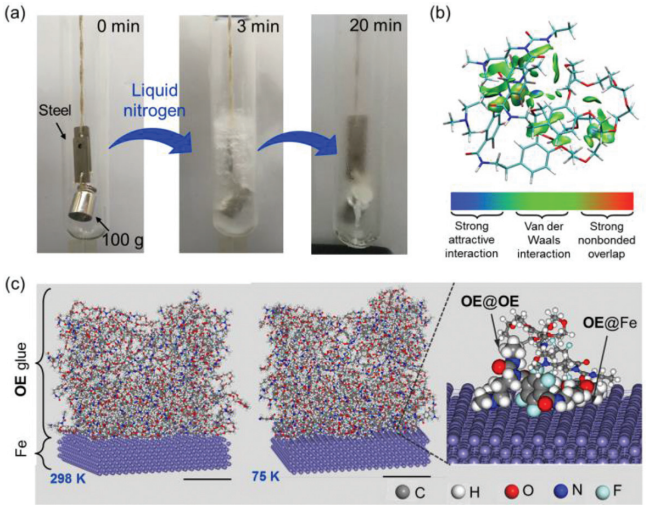

Fig. 4. Supramolecular adhesion behavior of **OE** at low temperatures. (a) Adhesion behavior of **OE** in liquid nitrogen. (b) The independent gradient model (IGM) isosurfaces for the interaction of **OE** and **OE** in a molar ratio of 1:1. (c) Molecular dynamic simulation of configurations of the molecular model of **OE** and steel (with Fe atom as model) at 298 K and 77 K, respectively. The scale bar represents 2 nm.

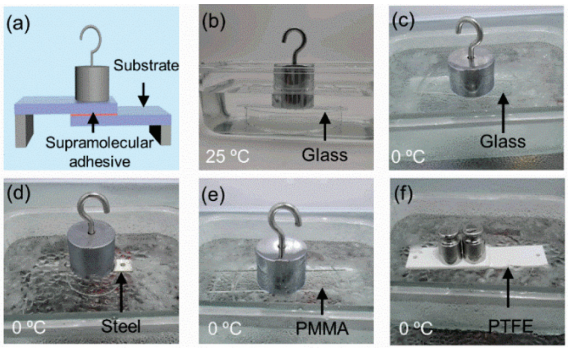

Fig. 5. Underwater adhesion performance of **OE**. (a) Schematic diagram of underwater adhesion of **OE**. (b-f) Macroscopic underwater adhesion behavior of **OE** to various substrates, including glass piece (b, c), steel piece (d), PMMA piece (e), and PTFE piece (f). Two weights are 500 g and 100 g, respectively.

adhered together in liquid nitrogen by **OE**. Meanwhile, good adhesion of **OE** was also observed when testing temperature was quickly increased from −196 °C to 25 °C. Lap-shear tests clearly proved the good adhesion effect of **OE** to steel in liquid nitrogen, with the adhesion strength at 0.87 MPa (Fig. S33 in Supporting information). No obvious decay of interaction energy between **OE** and steel was observed as the temperature was decreased from 298 K to 77 K. Similar result was found from cohesive energy density (CED, cohesion effect) of **OE**. The simulation model clearly showed the non-covalent interactions in adhesion and cohesion steps of the bulk **OE** cluster to iron surface. These simulation results are fully consistent with the macroscopic adhesion behavior of **OE** (Figs. 4b and c, Figs. S35−S43 and Tables S1−S3 in Supporting information).

With the abovementioned adhesion behavior of **OE** in mind, underwater adhesion tests at low temperatures were designed and carried out. No separation or displacement of adhered steel by **OE** was found, when the adhesion was taken place in the presence of water (Fig. 5d). Similar observations were recorded in the underwater weight-loading tests. Changing the surfaces from steel to glass, PMMA or PTFE, did not exert obviously influences on the adhesion effects of **OE** (Fig. 5). When the water temperature was cooled to 0 °C (in an ice-water bath), tough adhesion behaviors of **OE** to four tested surfaces were still successfully achieved.

As shown in Fig. S34 (Supporting information), the average adhesion strength of **OE** (in an ice-water bath) at 2.73 and 2.84 MPa on steel and glass are observed, respectively. Similarly, good adhesion ability of **OE** was obtained, when steel or glass was replaced by other testing substrates (PMMA or PTFE). Although moderate decay in adhesion strength was observed along with prolonged soaking time, tough adhesion of **OE** to glass and PMMA was still obtained under water.

In conclusion, a low-molecular-weight supramolecular adhesive was serendipitously obtained. Tough and long-term adhesion of **OE** to diverse substrates at low temperatures (from −4 °C to −80 °C) was successfully realized. Compared with traditional adhesive materials with good resistance to low temperatures, **OE** did not have any anti-freeze components. **OE** exhibited excellent resistance to low temperatures (including extremely low temperatures). Moreover, **OE** showed a potential as an underwater adhesive material. This work not only enriches the family of supramolecular adhesives, but also is helpful for designing low temperature-resistance adhesive materials.

Declaration of competing interest

The authors declare that they have no known competing financial interests or personal relationships that could have appeared to influence the work reported in this paper.

Acknowledgments

The authors gratefully acknowledge the Outstanding Youth Scientist Foundation of Hunan Province (No. 2021JJ10010), the Huxiang Young Talent Program from Hunan Province (No. 2018RS3036), the Fundamental Research Funds for the Central Universities from Hunan University. Moreover, this work is supported by the Hunan Provincial Innovation Foundation for Postgraduate (No. CX20200446).

Supplementary materials

Supplementary material associated with this article can be found, in the online version, at doi:10.1016/j.cclet.2022.107830.

References

[1] J. Courtois, I. Baroudi, N. Nouvel, et al., Adv. Funct. Mater. 20 (2010) 1803–1811.
[2] S.J. Cheng, M.Q. Zhang, N. Dixit, R.B. Moore, T.E. Long, Macromolecules 45 (2012) 805–812.
[3] C. Heinzmann, C. Weder, L.M. de Espinosa, Chem. Soc. Rev. 45 (2016) 342–358.
[4] C.Y. Shi, Q. Zhang, H. Tian, D.H. Qu, SmartMat 1 (2020) e1012.
[5] Y. Zhao, S.L. Song, X.Z. Ren, et al., Chem. Rev. 122 (2022) 5604–5640.
[6] Q. Zhang, C.Y. Shi, D.H. Qu, et al., Sci. Adv. 4 (2018) eaat8192.
[7] S.H. Mostafavi, F. Tong, T.W. Dugger, D. Kisailus, C.J. Bardeen, Macromolecules 51 (2018) 2388–2394.
[8] X.F. Ji, M. Ahmed, L.L. Long, et al., Chem. Soc. Rev. 48 (2019) 2682–2697.
[9] W. Zhang, Y. Luo, J. Zhao, et al., Chin. Chem. Lett. 33 (2022) 2455–2458.
[10] B. Zhao, L. Jiang, Q. Jiang, Chin. Chem. Lett. 33 (2022) 11–21.
[11] C.A. Anderson, A.R. Jones, E.M. Briggs, et al., J. Am. Chem. Soc. 135 (2013) 7288–7295.
[12] D.L. Gan, W.S. Xing, L.L. Jiang, et al., Nat. Commun. 10 (2019) 1487.
[13] J.Y. Chen, D.W. Guo, S.H. Liang, Z.Z. Liu, Polym. Chem. 11 (2020) 6670–6680.
[14] M.G. Mazzotta, A.A. Putnam, M.A. North, J.J. Wilker, J. Am. Chem. Soc. 142 (2020) 4762–4768.
[15] S.G. Wu, C.Y. Cai, F.F. Li, Z.J. Tan, S.Y. Dong, CCS Chem. 2 (2020) 1690–1700.
[16] X. Li, Z.L. Wang, W. Li, J.Q. Sun, ACS Mater. Lett. 3 (2021) 875–882.
[17] M.W.M. Tan, G. Thangavel, P.S. Lee, Adv. Funct. Mater. 31 (2021) 2103097.
[18] C.Y. Cai, S.G. Wu, Z.J. Tan, F.F. Li, S.Y. Dong, ACS Appl. Mater. Interfaces 13 (2021) 53083–53090.
[19] H. Xu, X.Y. Jiang, X.S. Han, H.Z. Cai, F. Gao, J. Mater. Chem. A 9 (2021) 25104–25113.
[20] S. Xia, Y.K. Chen, J.F. Tian, et al., Adv. Funct. Mater. 31 (2021) 2101143.
[21] D.W.R. Balkenende, C.A. Monnier, G.L. Fiore, C. Weder, Nat. Commun. 7 (2016) 10995.

[22] A. Lavrenova, D.W.R. Balkenende, Y. Sagara, et al., J. Am. Chem. Soc. 139 (2017) 4302–4305.
[23] J. Courtois, I. Baroudi, N. Nouvel, et al., Adv. Funct. Mater. 20 (2010) 1803–1811.
[24] C. Heinzmann, U. Salz, N. Moszner, G.L. Fiore, C. Weder, ACS Appl. Mater. Interfaces 7 (2015) 13395–13404.
[25] X. Li, N. Mignard, M. Taha, et al., Macromolecules 52 (2019) 6585–6599.
[26] H.B. Gao, X.D. Ma, J.P. Lin, et al., Macromolecules 52 (2019) 7731–7739.
[27] R.D. Adams, V. Mallick, J. Adhes. 43 (1993) 17–33.
[28] S.G. Kang, M.G. Kim, C.G. Kim, Compos. Struct. 78 (2007) 440–446.
[29] J.J.M. Machado, E.A.S. Marques, L.F.M. da Silva, Compos. Struct. 194 (2018) 68–79.
[30] J.J. Xu, R.J. Jing, X.Y. Ren, G.H. Gao, J. Mater. Chem. A 8 (2020) 9373–9381.
[31] X. Li, J.L. Lai, Y. Deng, et al., J. Am. Chem. Soc. 142 (2020) 21522–21529.
[32] X. Su, H. Wang, Z.L. Tian, et al., ACS Appl. Mater. Interfaces 12 (2020) 29757–29766.
[33] L. Wu, L.W. Li, M.J. Qu, H. Wang, Y.Z. Bin, ACS Appl. Polym. Mater. 2 (2020) 3094–3106.
[34] Y. Yao, Z.Y. Xu, B. Liu, et al., Adv. Funct. Mat. 31 (2021) 2006944.
[35] Y.J. Chen, Y.N. Zhang, A. Mensaha, et al., Carbohydr. Polym. 255 (2021) 117508.
[36] J. Wen, J. Tang, H.M. Ning, et al., Adv. Funct. Mater. 31 (2021) 2011176.
[37] S.G. Wu, Q. Zhang, Y. Deng, et al., J. Am. Chem. Soc. 142 (2020) 448–455.
[38] J. Watte, W. van Gompel, P. Lemmens, et al., ACS Appl. Mater. Interfaces 8 (2016) 29759–29769.
[39] S.Y. Dong, J. Leng, Y.X. Feng, et al., Sci. Adv. 3 (2017) eaao0900.
[40] Q. Zhang, T. Li, A.B. Duan, et al., J. Am. Chem. Soc. 141 (2019) 8058–8063.
[41] X. Li, Y. Deng, J.L. Lai, G. Zhao, S.Y. Dong, J. Am. Chem. Soc. 142 (2020) 5371–5379.
[42] Q.F. Rong, W.W. Lei, L. Chen, et al., Angew. Chem. Int. Ed. 56 (2017) 14159–14163.
[43] S.W. Hao, L. Meng, Q.J. Fu, F. Xu, J. Yang, Chem. Eng. J. 431 (2022) 133782.
[44] Y. Deng, X. Li, C. Han, S.Y. Dong, Chin. Chem. Lett. 31 (2020) 3221–3224.
[45] M.M. Zhang, X.Z. Yan, F.H. Huang, Z.B. Niu, H.W. Gibson, Acc. Chem. Res. 47 (2014) 1995–2005.
[46] Z. Wu, C.D. Ji, X.J. Zhao, et al., J. Am. Chem. Soc. 141 (2019) 7385–7390.
[47] D.K. Hohl, C. Weder, Adv. Opt. Mater. 7 (2019) 1900230.
[48] T. Xiao, L. Zhou, X.Q. Sun, et al., Chin. Chem. Lett. 31 (2020) 1–9.
[49] Q. Xu, Z. Cui, J. Yao, et al., Chin. Chem. Lett. 32 (2021) 4024–4028.
[50] X. Zhao, Y. Liu, Z.Y. Zhang, et al., Angew. Chem. Int. Ed. 60 (2021) 17904–17909.